

Identifying Parameter-Dependent Volterra Kernels to Predict Aeroelastic Instabilities

Rick Lind*

University of Florida, Gainesville, Florida 32611

Richard J. Prazenica[†] and Martin J. Brenner[‡]

NASA Dryden Flight Research Center, Edwards, California 93523

and

Dario H. Baldelli[§]

ZONA Technology, Scottsdale, Arizona 85251

Flight testing for envelope expansion remains dangerous and costly because of difficulties in accurately predicting the onset of flutter. Approaches have been developed that are able to identify optimal models of the aeroelastic dynamics based on flight data but are not able to predict the responses at all airspeeds. Those previous approaches are extended to include parameter variations in the optimal models. Specifically, parameter-varying models of Volterra kernels are identified for inclusion with theoretical models in aeroelastic analysis. The new approach is applied to a pitch-plunge system to demonstrate the accuracy achieved in predicting the onset of flutter by analyzing data obtained at lower airspeeds.

Nomenclature

C	=	structural damping matrix
D	=	aerodynamic stiffness matrix
E	=	aerodynamic damping matrix
F	=	input matrix
F_l	=	linear fractional transformation
f	=	function
h	=	Volterra kernel
K	=	structural stiffness matrix
M	=	structural mass matrix
P	=	plant with airspeed dependency
\bar{P}	=	plant with airspeed parameterization
Q	=	unsteady force matrix
\bar{q}	=	dynamic pressure
U	=	airspeed
u	=	input vector
w	=	signal
X	=	unknown dynamics with airspeed dependency
\bar{X}	=	unknown dynamics with airspeed parameterization
x	=	state vector
y	=	measurement vector
z	=	signal
δ_U	=	perturbation to airspeed
ζ	=	damping ratio
ω	=	natural frequency

I. Introduction

ACCURATE knowledge of the aeroelastic dynamics is required to predict airspeeds at which the onset of flutter will occur for an aircraft undergoing flight testing. Such accuracy is difficult to achieve using theoretically assumed dynamics or experimentally estimated models.¹ Approaches are being developed that inherently use both flight data and theoretical models to analyze stability of aeroelastic systems. Such approaches are beneficial because they are based on measured properties of the aircraft while retaining the structure of the theoretical equations of motion.

A fundamental approach called the μ -method analysis was developed for flutter prediction based on theoretical models and flight data.² Essentially, this approach uses flight data to indicate uncertainty in the theoretical model and then predict a worst-case flutter speed that is robust with respect to that uncertainty. Flight tests indicate this method is able to predict flutter speeds with a level of conservatism commensurate with the uncertainty. Unfortunately that uncertainty, and consequently the conservatism, can be significant so the approach restricts the flight envelope more than necessary.

The approach was augmented to include a prefilter analysis of the flight data using Volterra kernels.³ Such kernels are able to represent a variety of dynamic systems and have been shown to be especially practical for aeroelastic systems.^{4–9} The augmented approach computed Volterra kernels to represent the flight data such that linear and nonlinear components were separated. The kernels corresponding to the linear components of the flight data were then used to estimate uncertainty in a linearized model. The resulting flutter speeds were less conservative because the effects of unmodeled nonlinearities were eliminated; however, the approach still did not properly account for errors in the theoretical dynamics. This approach only added uncertainty to account for errors rather than updating the model to eliminate those errors.

A method to update the linearized dynamics was implemented that incorporated a modal parameter estimation to the flutterometer.¹⁰ This approach analyzed the properties of the Volterra kernel associated with linear components of the data to identify the underlying dynamics. In particular, the dynamics at frequencies associated with the aeroelastic modes were used to identify parameters of natural frequency and damping. The theoretical model was updated to include these parameters, and the conservatism in the resulting flutter speeds was indeed reduced; however, the updating assumed corrections only to static parameters of the model,

Presented as Paper 2004-1517 at the AIAA Structures, Structural Dynamics, and Materials Conference, Palm Springs, CA, 19–22 April 2004; received 6 July 2004; revision received 1 June 2005; accepted for publication 29 July 2005. Copyright © 2005 by Rick Lind. Published by the American Institute of Aeronautics and Astronautics, Inc., with permission. Copies of this paper may be made for personal or internal use, on condition that the copier pay the \$10.00 per-copy fee to the Copyright Clearance Center, Inc., 222 Rosewood Drive, Danvers, MA 01923; include the code 0001-1452/05 \$10.00 in correspondence with the CCC.

*Assistant Professor, Department of Mechanical and Aerospace Engineering, 231 Aerospace Building; ricklind@ufl.edu. Senior Member AIAA.

[†]National Research Council Fellow, MS 4840; chad.prazenica@dfrc.nasa.gov. Member AIAA.

[‡]Research Engineer, MS 4840, Aerostructures Branch; martin.j.brenner@nasa.gov. Member AIAA.

[§]Control Engineering Specialist, 7430 E. Stetson Drive, Suite 205; dario@zonatech.com. Member AIAA.

which do not change as airspeed changes. The approach only updated modal parameters of the structural dynamics and was not able to properly account for errors that are dependent on airspeed nor properly account for unmodeled dynamics.

The approach was extended to account for the problem of unmodeled dynamics by identifying an operator that correlates to unknown dynamics.¹¹ This approach used higher-order Volterra kernels to account for errors and unmodeled dynamics associated with linear and nonlinear dynamics. Unfortunately, this extended approach also assumed static updates and was not able to account for the dependency on airspeed of the unknown dynamics. The resulting model accurately predicted the responses at a given flight condition but was unable to predict the stability at a different flight condition.

This paper introduces parameter-varying models of the Volterra kernels to account for the unknown dynamics. Basically, the unknown dynamics are identified as Volterra kernels, using the previous procedure, at a set of flight conditions, and then a state-space model with airspeed dependency is computed to represent those kernels. The resulting model is able to predict the measured responses at current and future airspeeds during a flight test.

An example is presented to demonstrate the procedure involving these parameter-dependent Volterra kernels. This example simulates response data taken from a standard pitch–plunge model whose dynamics are not entirely known. The system is restricted to linear dynamics such that only first-order kernels are needed to account for the modeling errors. The procedure can be extended to consider higher-order kernels; however, the restriction to first-order kernels allows the concept to be sufficiently presented and explained. Also, procedures do not currently exist that can properly compute a stability margin with respect to parameter-dependent second-order kernels whereas the μ -method analysis can be directly applied to parameter-dependent first-order kernels.

II. Concept

A. Formulation

The basic representation of an aeroelastic system under consideration is given in Eq. (1):

$$M\ddot{x} + C\dot{x} + Kx + \bar{q}Qx - Fu = X(z) \quad (1)$$

This general formulation uses $x \in \mathcal{R}^{n_x}$ as the modal displacement vector and $u \in \mathcal{R}^{n_u}$ as the input vector. The dynamics are described by $M \in \mathcal{R}^{n_x \times n_x}$ as the structural mass matrix, $C \in \mathcal{R}^{n_x \times n_x}$ as the structural damping matrix, $K \in \mathcal{R}^{n_x \times n_x}$ as the structural stiffness matrix, $F \in \mathcal{R}^{n_x \times n_u}$ as the input matrix, $Q \in \mathcal{R}^{n_x \times n_x}$ as the unsteady aerodynamic force matrix, and \bar{q} as the dynamic pressure. Also, the element $X: \mathcal{R}^{n_z} \rightarrow \mathcal{R}^{n_x}$ is dimensioned as a mapping between $z \in \mathcal{R}^{n_z}$ and the states.

The function $X(z)$ represents an unknown, possibly nonlinear, contribution to the dynamics. This mapping may represent errors in the linear model or unmodeled nonlinearities. The element is described as a function of the states and inputs whose linear combination is described by z .

The dynamics in Eq. (1) can be expressed as a pair of operators that are related by feedback.¹¹ Such an expression essentially separates the known from unknown dynamics to facilitate identification of these unknown dynamics. The operator used to represent the known dynamics can be realized as a state-space model; however, the actual model cannot be written without knowing the exact finite-state representation of the unsteady aerodynamic force.¹² A suitable finite-state representation can generally be found such that operators \bar{P} and \bar{X} can be formulated and related as in Fig. 1.¹¹

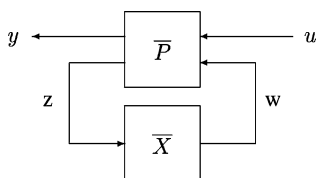


Fig. 1 Feedback relationship of operators.

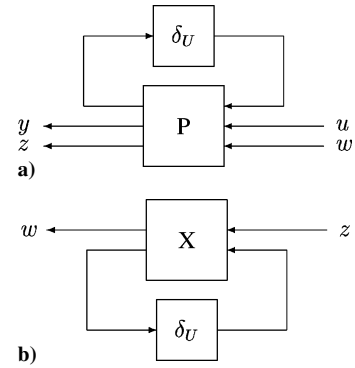


Fig. 2 Parameterized models of a) known and b) unknown dynamics.

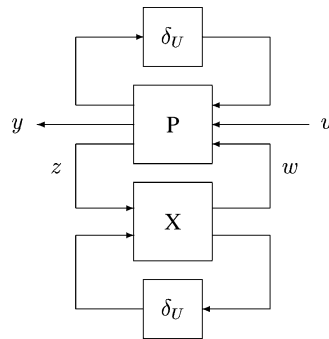


Fig. 3 Block diagram.

An aeroelastic system is described by the known dynamics in Fig. 1 along with an appropriate operator for the unknown dynamics. A procedure was formulated to compute optimal estimates of these unknown dynamics¹¹; however, that procedure only accounted for the dynamics at a given value of airspeed. In reality, both the known dynamics and unknown dynamics will vary with airspeed.

The dynamics can be parameterized around airspeed by introducing a perturbation δ_U to a nominal airspeed U_o such that $U = U_o + \delta_U$. The known dynamics and unknown dynamics can then be expressed as in Fig. 2 by using standard operations.¹³

The aeroelastic system represented in Fig. 3 results from combining the relationship in Fig. 1 with the parameterization in Fig. 2.

B. Optimal Estimates

Optimal estimates for the unknown dynamics are needed to ensure the model in Fig. 3 can accurately predict the stability of the true system. These optimal estimates are computed by comparing measured responses and predicted responses. In this way, the unknown dynamics are determined from flight data.

A simplified notation is used to describe the dynamics at a particular airspeed. The notation F_l is used to describe two operators that are related through the lower loop, and F_u is used to describe two operators that are related through the upper loop. In this way, the known dynamics in Fig. 2 are described by $[y, z] = F_u(P, \delta_U)[u, w]$, and the unknown dynamics are described by $w = F_l(X, \delta_U)z$.

Furthermore, the notation indicates dynamics and associated responses at distinct airspeeds. Let y^i represent the predicted response and \bar{y}^i represent the measured response at airspeed of U^i . Note this airspeed corresponds to a perturbation of $\delta_U^i = U^i - U_o$ for a model that is formulated at the nominal airspeed of U_o .

Define $\bar{P}^i = F_u(P, \delta_U^i)$ as the known dynamics and $\bar{X}^i = F_l(X, \delta_U^i)$ as the unknown dynamics that are related as in Fig. 2. In this case, these elements represent the known dynamics and unknown dynamics at the airspeed of U^i .

The derivation of the identification procedure is simplified by considering a particular representation of \bar{P}^i . This model can be presented as a matrix of transfer functions. In this case, \bar{P}^i is described as matrix of four transfer functions relating the two inputs

to the two outputs:

$$\bar{P}^i = \begin{bmatrix} \bar{P}_{11}^i & \bar{P}_{12}^i \\ \bar{P}_{21}^i & \bar{P}_{22}^i \end{bmatrix} \quad (2)$$

The unknown operator $\bar{X}^i(z)$ can be identified as a mapping between the z and w signals. As such, these signals must be isolated. Such an isolation can be accomplished using the elements \bar{P}_{11}^i and \bar{P}_{12}^i of the transfer function matrix. These elements are used to compute the expected output measurements of the model by noting that $w = \bar{X}^i(z)$ in Fig. 1:

$$y^i = \bar{P}_{11}^i x + \bar{P}_{12}^i \bar{X}^i(z) \quad (3)$$

The operator is chosen such that the expected output of the model, y^i , matches the measurements from the system, \bar{y}^i , acquired by flight data. Consequently, the unknown element can be identified as an optimization:

$$\bar{X}^i = \arg \min_f \|\bar{y}^i - \bar{P}_{11}^i x - \bar{P}_{12}^i f(z)\| \quad (4)$$

This formulation in Eq. (4) is a particularly attractive approach for flight-test programs. Essentially, the minimization is based on the difference between measured and simulated data. The measurement data \bar{y}^i represents the nonlinear system and the simulated data $\bar{P}_{11}^i x$ represents the linearized model.

The approach needs to be augmented to account for the nominal value of the unknown dynamics X that is independent of the airspeed through the relationship $\bar{X}^i = F_i(X, \delta_U^i)$. This value is computed by extending the minimization to account for multiple airspeeds as in Eq. (5):

$$X = \arg \min_f \sum_i \|\bar{y}^i - \bar{P}_{11}^i x - \bar{P}_{12}^i F_i(f, \delta_U^i)\| \quad (5)$$

A representation for $X(z)$ can be computed as a set of Volterra kernels. These kernels allow linear and nonlinear elements of the unknown dynamics to be identified. Of course, several techniques for system identification can be applied but this paper restricts attention to Volterra kernels.

III. Volterra Kernels

A. Formulation

Volterra series representations provide a convenient framework for the analysis of nonlinear dynamic systems. The Volterra theory of nonlinear systems states that the system output w can be expressed in terms of an infinite series of integral operators of increasing order^{14,15}:

$$w(t) = w_1(t) + w_2(t) + \dots + w_\infty(t) \quad (6)$$

In practice, the series is often truncated to include only the first-order and second-order operators. For a causal, time-invariant, single-input/single-output system, these operators take the form in Eqs. (7) and (8):

$$w_1(t) = \int_0^t h_1(\xi) z(t - \xi) d\xi \quad (7)$$

$$w_2(t) = \int_0^t \int_0^t h_2(\xi, \eta) z(t - \xi) z(t - \eta) d\xi d\eta \quad (8)$$

The input is denoted as z , and h_1 and h_2 denote the first-order and second-order Volterra kernels. Collectively, the Volterra kernels provide a model of the system, because once the kernels have been identified, the response to any arbitrary input can be determined. The first-order kernel represents the linear dynamics of the system, and the higher-order kernels characterize the nonlinear dynamics. It should be noted that, for a linear system, the first-order kernel is equivalent to the impulse response of the system, and the output

is given by Eq. (7). Therefore, the Volterra theory can be viewed as an extension of the concept of linear convolution to nonlinear systems.

B. First-Order Parameter-Varying Expression

The kernels as expressed in Eqs. (7) and (8) are expressed only as a function of time. As such, they are formulated to represent the aeroelastic dynamics at a constant flight condition. Models must be derived that can represent these kernels but also retain information about the variation with airspeed for the associated dynamics. The derivation here is restricted to only the first-order kernel because finite-state representations are easily derived for flutter analysis.

A straightforward approach simply notes how the function comprising the kernel varies with airspeed. Such an approach uses, a first-order kernel as $h_1(\xi, U)$. The computation of the kernel could then be computed by curve fit to the kernels computed at various airspeeds. This approach is relatively easy to implement, but the resulting kernel still needs to be represented in a fashion suitable for state-space modeling and μ -method analysis.

An alternative approach first computes state-space representations of the unknown dynamics at a set of airspeeds and then finds a parameter-varying model to encompass those representations. This approach ensures the resulting model is directly applicable to μ -method analysis to predict the onset of flutter. Define the model, \bar{P}^i , as the unknown dynamics at airspeed of U^i and restrict the derivation to first-order systems for convenience:

$$w^i = w_1^i(t) \quad (9)$$

$$= \int_0^t h_1(\xi) z(t - \xi) d\xi \quad (10)$$

$$= \bar{P}^i z^i \quad (11)$$

A parameter-varying model of the unknown dynamics can be computed by directly varying a transfer function based on values of \bar{P}^i at different airspeeds. Such a model is formulated by directly relating a set of transfer functions to the unknown dynamics as in Eq. (13):

$$w^i = \bar{P}^i z^i \quad (12)$$

$$= [P_o + P_1 U^i + P_2 (U^i)^2] z^i \quad (13)$$

A parameter-varying model can also be computed by varying the elements of a state-space model. Essentially, the transfer function in Eq. (13) can be expressed as a state-space model formed by a matrix quadruple. Each of these matrices can be written as a function of airspeed and combined to generate a parameter-varying state-space model as in Eq. (16):

$$w^i = \bar{P}^i z^i \quad (14)$$

$$= \begin{bmatrix} \bar{A}^i & \bar{B}^i \\ \bar{C}^i & \bar{D}^i \end{bmatrix} z^i \quad (15)$$

$$= \begin{bmatrix} A_o + A_1 U^i + A_2 (U^i)^2 & B_o + B_1 U^i + B_2 (U^i)^2 \\ C_o + C_1 U^i + C_2 (U^i)^2 & D_o + D_1 U^i + D_2 (U^i)^2 \end{bmatrix} z^i \quad (16)$$

IV. Stability Analysis

Flutter speeds of the aeroelastic dynamics are predicted by analyzing stability of the system in Fig. 3. A stability margin is the smallest perturbation to airspeed, δ_U^* , which results in the onset of flutter. Such a margin is computed from a minimization using Eq. (17) as applied to the system in Fig. 3:

$$\delta_U^* = \min_{\delta_U} \text{ such that } F_1(F_u(P, \delta_U), F_l(X, \delta_U)) \text{ is unstable} \quad (17)$$

The flutter speed corresponds to $U^* = U_o + \delta_U^*$. Such a speed is also considered the critical flutter speed because it represents the

Table 1 System parameters

Parameter	Value
a	-0.6
b	0.135 m
m	12.387 kg
k_α	2.82 Nm/rad
c_α	0.180 m ² kg/s
c_{l_α}	6.28
c_{l_β}	3.358
I_α	0.065 m ² kg
ρ	1.225 kg/m ³
x_α	0.2466
k_h	2844.4 N/m
c_h	27.43 kg/s
c_{m_α}	-0.628
c_{m_β}	-0.635

lowest speed at which a mode becomes unstable. The formulation in Eq. (17) can easily be extended to compute subcritical flutter speeds corresponding to perturbations at which the system has multiple unstable modes.

Also, the problem in Eq. (17) can be written in the format of the structured singular value for systems in which P and X are linear. In this case, the elements are expressed as state-space systems, and the tools for robust analysis are directly applied.

V. Example

A. System

The process of estimating a model to describe aeroelastic dynamics is applied to a pitch-plunge system. This system is composed of a rigid airfoil, whose motion is restricted to pitching and plunging, mounted in a wind tunnel. This model is not necessarily reflective of a physical system; rather, it presents a representative model for simulating an envelope expansion. The dynamics used as a truth model for this simulation are shown in Eq. (18):

$$\begin{aligned} & \begin{bmatrix} m & mx_\alpha b \\ mx_\alpha b & I_\alpha \end{bmatrix} \begin{bmatrix} \ddot{h} \\ \ddot{\alpha} \end{bmatrix} + \begin{bmatrix} c_h & 0 \\ 0 & c_\alpha \end{bmatrix} \begin{bmatrix} \dot{h} \\ \dot{\alpha} \end{bmatrix} + \begin{bmatrix} k_h & 0 \\ 0 & k_\alpha \end{bmatrix} \begin{bmatrix} h \\ \alpha \end{bmatrix} \\ & = \rho U^2 b s \begin{bmatrix} -c_{l_\alpha} [\alpha + (1/U)\dot{h} + (\frac{1}{2} - a)b(1/U)\dot{\alpha}] - c_{l_\beta} \beta \\ c_{m_\alpha} b [\alpha + (1/U)\dot{h} + (\frac{1}{2} - a)(b/U)\dot{\alpha}] + c_{m_\beta} b \beta \end{bmatrix} \end{aligned} \quad (18)$$

These dynamics describe the complete aeroelastic system. The degrees of freedom of the rigid airfoil are described by the plunge h and the pitch α parameters. The left side of the equality describes the structural dynamics, and the right side of the equality describes the quasi-steady aerodynamics that are generated in response to motion of the airfoil and commanded rotations β a flap.

The parameters describing the dynamics of the system are given in Table 1. These parameters are generally indicative of those presented

fairly traditional with the two modes coalescing in natural frequency as damping becomes unstable.

B. Model

A model is generated to approximate the dynamics of the pitch-plunge system. This model represents a best-guess approximation of the true dynamics as is commonly generated for any flutter analysis. In this case, the model has the correct equations of motion to describe the simulated truth model but an incorrect coefficient for torsional stiffness as indicated by the model parameters: true $k_\alpha = 2.82$ and model $k_\alpha = 2.26$. The parameter-varying Volterra kernels are used to identify this error and predict an accurate value of flutter speed.

The formulation of the model uses several matrices to simplify the notation. These matrices are generated by using the definitions in Eq. (19):

$$\begin{aligned} M &= \begin{bmatrix} m & mx_\alpha b \\ mx_\alpha b & I_\alpha \end{bmatrix}, & C &= \begin{bmatrix} c_h & 0 \\ 0 & c_\alpha \end{bmatrix}, & K &= \begin{bmatrix} k_h & 0 \\ 0 & k_\alpha \end{bmatrix} \\ D &= \begin{bmatrix} 0 & -c_{l_\alpha} \rho b \\ 0 & c_{m_\alpha} \rho b^2 \end{bmatrix}, & E &= \begin{bmatrix} -c_{l_\alpha} \rho b & -c_{l_\alpha} \rho b^2 (0.5 - a) \\ c_{m_\alpha} \rho b^2 & c_{m_\alpha} \rho b^3 (0.5 - a) \end{bmatrix} \\ & & F &= \begin{bmatrix} -c_{l_\beta} \rho b \\ c_{m_\beta} \rho b^2 \end{bmatrix} \end{aligned} \quad (19)$$

The equation of motion, including an unknown dynamic, is written in Eq. (20) using these matrix definitions and the state vector defined as $x = [h, \alpha]$:

$$M\ddot{x} + C\dot{x} + Kx + X = U^2 D\dot{x} + U E\dot{x} + U^2 F\beta \quad (20)$$

The model needs to be expressed in a form that includes feedback relationships between the known dynamics and the unknown dynamics along with a perturbation to airspeed. The derivation of the required expression is accomplished by introducing the pairs of signals, defined in Eqs. (21–24), to the dynamics. Also, the airspeed is replaced with a nominal value plus perturbation as $U = U_o + \delta_U$:

$$z_x = x, \quad w_x = X(z_x) \quad (21)$$

$$z_1 = 2U_o D\dot{x} + E\dot{x} + 2U_o F\beta, \quad w_1 = \delta_U z_1 \quad (22)$$

$$z_2 = D\dot{x} + F\beta, \quad w_2 = \delta_U z_2 \quad (23)$$

$$z_3 = w_2, \quad w_3 = \delta_U z_3 \quad (24)$$

These definitions allow Eq. (20) to be written as Eq. (25):

$$M\ddot{x} = (U_o^2 D - K)x + (U_o E - C)\dot{x} + U_o^2 F\beta - w_x + w_1 + w_3 \quad (25)$$

The final plant model P is expressed in state-space form in Eq. (26). Note the vector $e = [0 \ 1]$ is used such that $ex = \alpha$. The resulting model interacts with the unknown dynamics X and the perturbation to airspeed δ_U as in Fig. 3. The first set of inputs and outputs, as grouped by brackets, are the signals relating P to δ_U . The second set of inputs and outputs correlate to the input command and sensor measurements. The third set of inputs and outputs relate P to X :

$$P = \left[\begin{array}{cc|cc} 0 & I & [0 \ 0 \ 0] & 0 & 0 \\ M^{-1}(U_o^2 D - K) & M^{-1}(U_o E - C) & [M^{-1} \ 0 \ M^{-1}] & M^{-1} U_o^2 F & -M^{-1} e^T \\ \hline \begin{bmatrix} 2U_o D \\ D \\ 0 \end{bmatrix} & \begin{bmatrix} E \\ 0 \\ 0 \end{bmatrix} & \begin{bmatrix} 0 & 0 & 0 \\ 0 & 0 & 0 \\ 0 & I & 0 \end{bmatrix} & \begin{bmatrix} 2U_o F \\ F \\ 0 \end{bmatrix} & \begin{bmatrix} 0 \\ 0 \\ 0 \end{bmatrix} \\ I & 0 & [0 \ 0 \ 0] & 0 & 0 \\ e & 0 & [0 \ 0 \ 0] & 0 & 0 \end{array} \right] \quad (26)$$

in several references^{16,17}; however, the value of pitch damping has been increased simply to ensure the identified kernels decay within 4 s for ease of computation. The resulting flutter mechanism remains

C. Responses

Responses of the dynamics are simulated to illustrate the differences between the true system and assumed model. Volterra kernels

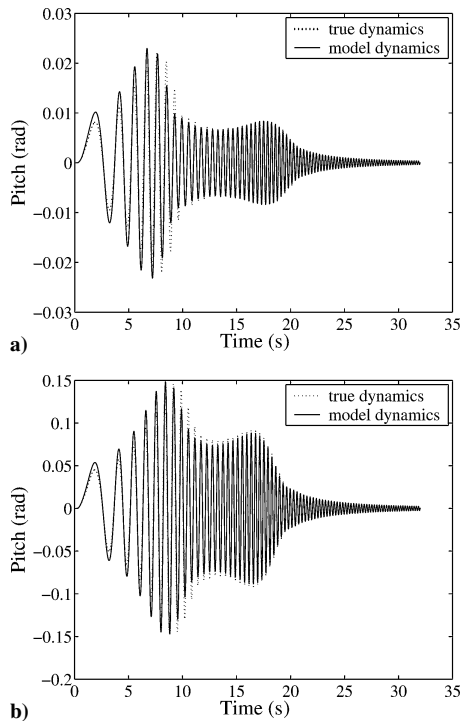


Fig. 4 Pitch angle in response to a chirp input at a) $U = 3$ m/s and b) $U = 8$ m/s.

are computed to represent these differences at various values of airspeed. In this way, the estimation process actually identifies the unknown dynamics in the model that account for the differences between measured and predicted responses.

A chirp signal is commanded to the flap to generate responses from the simulation. This chirp command ranges from 0.0 to 5.0 Hz over 32 s. The magnitude of this flap command is 10 deg. The signal was chosen to have a frequency range that encompasses the modal dynamics and a magnitude that excites those dynamics to generate large responses.

Responses are computed at airspeeds ranging from $U = 3$ m/s to $U = 11$ m/s. Consequently, a total of nine responses are computed. The values of pitch angle and plunge are simulated; however, only the pitch angle is used for data analysis. The plunge could be used also but the pitch angle is sufficient to provide information about the unknown dynamics.

The pitch angle in response to the chirp command is shown in Fig. 4 for airspeeds of $U = 3$ m/s and $U = 8$ m/s. As shown, the assumed dynamics of the model differ from what is considered the true dynamics. The model responses differ in both magnitude and period of oscillation from the true responses. This difference, for the simulated example, obviously results from the erroneous value of torsion stiffness used to generate the model.

The unknown dynamics in the model are estimated by analyzing the difference between predicted and actual response of the dynamics. This difference constitutes a measure of prediction error and is shown in Fig. 5.

Clearly the unknown dynamics associated with the model vary with airspeed. The error in the model is actually the static parameter of torsion stiffness; however, the parameter affects the modal properties of the model. The modal properties obviously change with airspeed so the unknown dynamics can also be considered as dependent on airspeed. The identification of unknown dynamics could be simplified in this particular case because the error is known to be static but, in general, such an assumption cannot be justified.

D. Volterra Kernels

Volterra kernels are identified to account for the unknown dynamics in the model of the aeroelastic system. In this case, the kernels are estimated as the mapping between the pitch angle and the error

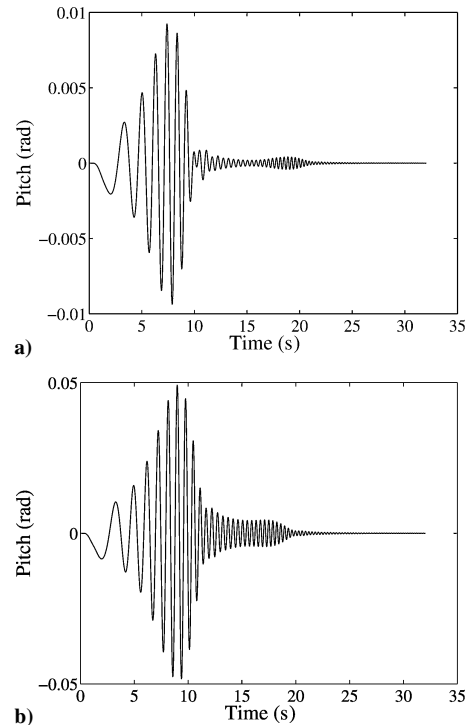


Fig. 5 Difference between predicted pitch angle and measured pitch angle at a) $U = 3$ m/s and b) $U = 8$ m/s.

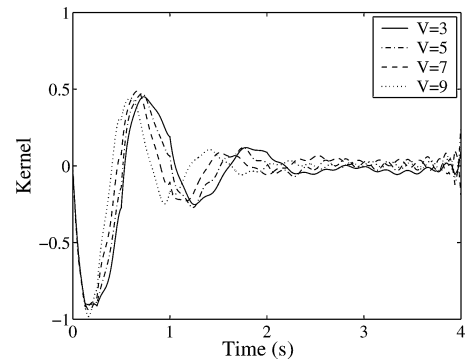


Fig. 6 Volterra kernels to represent the error in pitch angle at —, $U = 3$ m/s; ---, $U = 5$ m/s; - · - ·, $U = 7$ m/s; and · · · ·, $U = 9$ m/s.

in Fig. 5. The kernels represent the dynamics X that need to be added to the modeled dynamics as in Eq. (26) such that the modeled dynamics accurately predict the response of the true dynamics.

A set of kernels are computed to account for the unknown dynamics at airspeeds from $U = 3$ to 9 m/s. A separate kernel is computed, using the procedures previously documented,¹¹ at each airspeed. These kernels have the expected shapes of impulse responses as shown in Fig. 6.

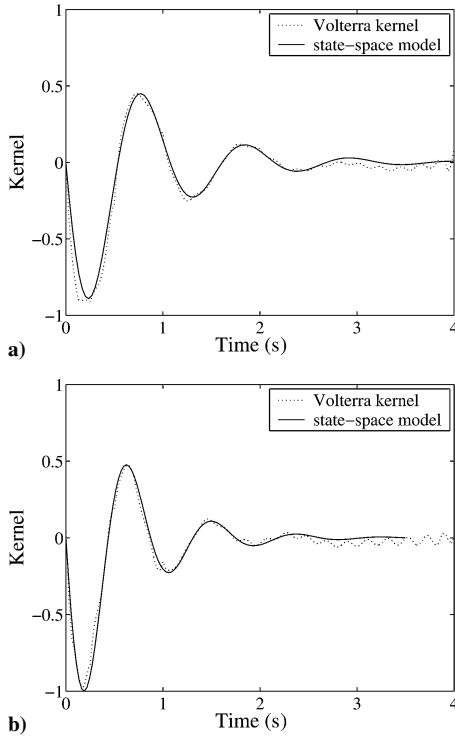
The error in predicted responses, shown in Fig. 5, and consequently the kernels representing the error, shown in Fig. 6, clearly demonstrate variation with airspeed. The most notable variation is a decrease in the period of the oscillations in the impulse response. The kernels are simply indicating that the modal frequency of the unknown dynamics is increasing as the airspeed increases. This increase in modal frequency correlates to the increase in natural frequency of the pitch mode as the system approaches flutter.

E. State-Space Representation of Kernels

State-space models are computed as finite-state representations of the Volterra kernels. In this case, the models are assumed to be single-mode models for each kernel. The basic form of the model uses a natural frequency ω , damping ζ , and magnitude α in the

Table 2 Modal properties of kernel representations

V	ω , rad/s	ζ	α
3	5.9841	0.2125	-0.2000
4	6.1002	0.1951	-0.1877
5	6.0415	0.1968	-0.2062
6	6.2210	0.2125	-0.2100
7	6.3467	0.2241	-0.2071
8	7.3920	0.2295	-0.1856
9	7.5701	0.2177	-0.1797
10	8.0554	0.2381	-0.1740

**Fig. 7** Volterra kernels and state-space representations for the unknown dynamics identified at a) $V = 3$ m/s and b) $V = 8$ m/s airspeeds.

formulation. The model \bar{X} is formulated in Eq. (27):

$$\bar{X} = \left[\begin{array}{cc|c} 0 & 1 & 0 \\ -\omega^2 & -2\zeta\omega & \alpha\omega^2 \\ \hline 1 & 0 & 0 \end{array} \right] \quad (27)$$

The impulse response of the unknown dynamics w is computed in Eq. (28):

$$w = \alpha(\omega/\sqrt{1-\zeta^2})e^{-\zeta\omega t} \sin(\omega\sqrt{1-\zeta^2}t) \quad (28)$$

Optimal parameters for the state-space models are computed using a least-squares fit. The resulting parameters, given in Table 2, illustrate variation with airspeed. The most noticeable variation is an increase in natural frequency with increase in airspeed. The remaining parameters of damping and magnitude scaling do not show any clear trends with airspeed.

The quality of these state-space models is demonstrated by comparing the impulse response of the state-space model and the actual kernel. Examples of such comparisons are shown in Fig. 7 and indicate the state-space models are reasonable representations of the Volterra kernels.

F. Parameter-Varying Representation

A parameter-varying model of the unknown dynamics is computed so that flutter speeds can be predicted. This model is formulated by assuming the dynamics vary quadratically with airspeed as

Table 3 Models and airspeeds

Model	Airspeed, m/s
X_5	$U \in \{3, 4, 5\}$
X_6	$U \in \{3, 4, 5, 6\}$
X_7	$U \in \{3, 4, 5, 6, 7\}$
X_8	$U \in \{3, 4, 5, 6, 7, 8\}$

in Eq. (29). The matrices are chosen as least-squares fit to the data in Table 2:

$$X = \left[\begin{array}{cc|c} A_0 + A_1U + A_2U^2 & B_0 + B_1U + B_2U^2 & \\ \hline [1 \ 0] & 0 & \end{array} \right] \quad (29)$$

The model needs to be parameterized around a nominal airspeed U_o by introducing a perturbation such that $U = U_o + \delta_U$. This parameterization results by relating the nominal model to the perturbation using the signals defined in Eqs. (30–32):

$$z_1 = (A_1 + 2A_2U_o)x + (B_1 + 2B_2U_o)u, \quad w_1 = \delta_U z_1 \quad (30)$$

$$z_2 = A_2x + B_2u, \quad w_2 = \delta_U z_2 \quad (31)$$

$$z_3 = w_2, \quad w_3 = \delta_U z_3 \quad (32)$$

These definitions allow Eq. (29) to be written in state-space form as in Eq. (33). This form interacts with the known dynamics as in Fig. 2:

$$X = \left[\begin{array}{cc|cc|cc} A_0 + A_1U_o + A_2U_o^2 & B_0 + B_1U_o + B_2U_o^2 & [I & 0 & I] \\ \hline [1 & 0] & 0 & [0 & 0 & 0] \\ \hline [A_1 + 2A_2U_o] & [B_1 + B_2U_o] & [0 & 0 & 0] \\ \hline [A_2] & [B_2] & [0 & 0 & 0] \\ \hline [0] & [0] & [0 & I & 0] \end{array} \right] \quad (33)$$

An envelope expansion is simulated with this model using the traditional concept of test points; namely, flutter speeds are predicted at each of a set of increasing airspeeds. At each airspeed, a parameter-varying model is computed based on a least-squares fit of the Volterra kernels identified at each previous airspeed. The models at test points of progressively increasing airspeeds are computed by accounting for the data measured at that airspeed along with data from the previous airspeeds. In this way, a set of parameter-varying models are computed such that each accounts for more information than was available to the previous. Define X_i as the parameter-varying model that is computed to account for data at airspeeds $U \leq i$ m/s as in Table 3.

The parameter-varying models are used to predict the unknown dynamics at any airspeed. As such, the objective is to analyze data from a set of airspeeds and predict the response at higher airspeeds. The predicted values of the unknown dynamics will not be identical to the actual values of the unknown dynamics because of errors in the identification and modeling process. Any difference between the predicted dynamics and actual dynamics will obviously cause error in the resulting prediction of flutter speeds.

The impulse response of the unknown dynamics at $U = 8$ m/s is computed using several parameter-varying models. Figure 8 shows the actual impulse response along with the predicted impulse responses from four models. These responses show the predictions clearly improve as more data are used to generate the unknown dynamics. The predicted response at $U = 8$ m/s that is generated using only data from $U \leq 5$ m/s is not as accurate as using data from $U \leq 7$ m/s. Actually, the predicted responses seem to converge to the actual response as the airspeed increases.

G. Flutter Prediction

Flutter speeds of the aeroelastic system are predicted during the simulated envelope expansion. Essentially, the best-guess model of

Table 4 Flutter speeds predicted by models with parameter-varying Volterra kernels

Model	Flutter speed, m/s
True	12.14
$F_l(P, 0)$	12.45
$F_l(P, X_5)$	9.64
$F_l(P, X_6)$	12.29
$F_l(P, X_7)$	12.29
$F_l(P, X_8)$	12.29
$F_l(P, X_9)$	12.29

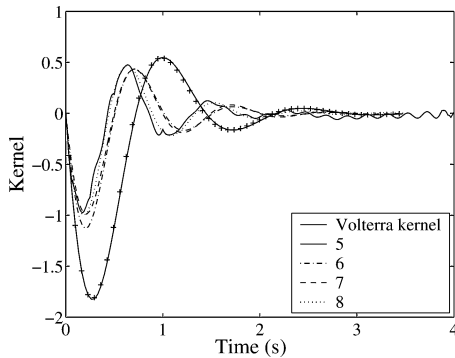


Fig. 8 Volterra kernel and predicted representations by using parameter-varying models of: +, X_5 ; ---, X_6 ; ----, X_7 and \cdots , X_8 for the unknown dynamics at $V = 8$ m/s.

the aeroelastic dynamics are coupled with the parameter-varying model of the unknown dynamics at a particular airspeed. Flutter speeds are predicted by computing the smallest perturbation to the resulting parameterized dynamics, which results in the onset of flutter.

The speeds at which flutter is predicted to occur are shown in Table 4. The best-guess model, with the inaccurate value of pitch stiffness, predicts a flutter speed higher than the true dynamics with about 2.55% error. The unknown dynamics are predicted using the parameter-varying representations of Volterra kernels and alter the flutter speeds. The speed predicted using data from $U \leq 5$ m/s predicts a flutter speed considerably different than the true flutter speed; however, the models generated using any data with $U > 5$ m/s are able to predict flutter speeds to within 1.23% of the true flutter speed.

Also, the computational requirements for this approach are reasonable in that all steps, including kernel estimation and stability analysis, can be performed within a minute on a desktop machine. That cost would increase if the amount of data, both number of channels and samples, were to increase significantly beyond the simple example. As such, the approach could potentially be implemented into current practices for online analysis during flight testing provided that only signals of prime importance would be evaluated.

VI. Conclusion

This paper presents a foundation by which Volterra kernels can be easily integrated into flutter prediction. Specifically, parameter-

varying models of Volterra kernels are introduced. Such models are sufficient to describe unknown, and possibly nonlinear, dynamics that vary as a function of airspeed. This approach allows models that are identified by updating theoretical dynamics to account for errors and unmodeled dynamics. The resulting parameter-varying models allow flutter speeds to be predicted using flight data from stable test points. A pitch-plunge model demonstrates that this approach is able to estimate unknown dynamics and alter the model to accurately predict the onset of flutter.

References

- ¹Keohoe, M. W., "A Historical Overview of Flight Flutter Testing," NASA TM-4720, Oct. 1995.
- ²Lind, R., and Brenner, M., "Flutterometer: An On-line Tool to Predict Robust Flutter Margins," *Journal of Aircraft*, Vol. 37, No. 6, 2000, pp. 1105–1112.
- ³Prazenica, R. J., Lind, R., and Kurdila, A. J., "Uncertainty Estimation from Volterra Kernels for Robust Flutter Analysis," *Journal of Guidance, Control, and Dynamics*, Vol. 26, No. 2, 2003, pp. 331–339.
- ⁴Silva, W., "Application of Nonlinear Systems Theory to Transonic Unsteady Aerodynamic Responses," *Journal of Aircraft*, Vol. 30, No. 5, 1993, pp. 660–668.
- ⁵Silva, W. A., and Bartels, R. E., "Development of Reduced-Order Models for Aeroelastic Analysis and Flutter Prediction Using the CFL3DV6.0 Code," *Journal of Fluids and Structures*, Vol. 19, No. 6, 2004, pp. 729–745.
- ⁶Marzocca, P., Librescu, L., and Silva, W. A., "Aeroelastic Response of Nonlinear Wing Sections Using a Functional Series Technique," *AIAA Journal*, Vol. 40, No. 5, 2002, pp. 813–824.
- ⁷Raveh, D. E., "Reduced-Order Models for Nonlinear Unsteady Aerodynamics," *AIAA Journal*, Vol. 39, No. 8, 2001, pp. 1417–1429.
- ⁸Lucia, D., and Beran, P. S., "Reduced-Order Model Development Using Proper Orthogonal Decomposition and Volterra Theory," *AIAA Journal*, Vol. 42, No. 6, 2004, pp. 1181–1190.
- ⁹Lucia, D. J., Beran, P. S., and Silva, W. A., "Reduced-Order Modeling: New Approaches for Computational Physics," *Progress in Aerospace Sciences*, Vol. 40, Feb. 2004, pp. 51–117.
- ¹⁰Lind, R., and Mortagua, J. P., "Accurate Flutterometer Predictions Using Volterra Modeling with Modal Parameter Estimation," *Journal of Aircraft*, Vol. 42, No. 4, 2005, pp. 998–1004.
- ¹¹Lind, R., Prazenica, R. J., and Brenner, M. J., "Estimating Nonlinearity Using Volterra Kernels in Feedback with Linear Models," AIAA Paper 2003-1406, 2003; also *Nonlinear Dynamics*, Vol. 39, No. 1, 2005, pp. 3–23.
- ¹²Karpel, M., "Design for Active Flutter Suppression and Gust Load Alleviation Using State-Space Aeroelastic Modeling," *Journal of Aircraft*, Vol. 19, No. 3, 1982, pp. 221–227.
- ¹³Lind, R., "Match-Point Solutions for Robust Flutter Analysis," *Journal of Aircraft*, Vol. 39, No. 1, 2002, pp. 91–99.
- ¹⁴Rugh, W. J., *Nonlinear System Theory: The Volterra–Wiener Approach*, Wiley, New York, 1980, pp. 1–70.
- ¹⁵Schetzen, M., *The Volterra and Wiener Theories of Nonlinear Systems*, Wiley, New York, 1980, pp. 11–49.
- ¹⁶Ko, J., Strganac, T. W., and Kurdila, A. J., "Stability and Control of a Structurally Nonlinear Aeroelastic System," *Journal of Guidance, Control, and Dynamics*, Vol. 21, No. 5, 1998, pp. 718–725.
- ¹⁷O'Neil, T., and Strganac, T. W., "Aeroelastic Response of a Rigid Wing Supported by Nonlinear Springs," *Journal of Aircraft*, Vol. 23, No. 4, 1998, pp. 616–622.

C. Pierre
Associate Editor